

Influence of F and Cl on the recrystallization of ion-implanted amorphous Si

I. Suni,^{a)} U. Shreter,^{b)} and M-A. Nicolet
California Institute of Technology, Pasadena, California 91125

J. E. Baker
Materials Research Laboratory, University of Illinois at Urbana-Champaign, Urbana, Illinois 61801

(Received 22 August 1983; accepted for publication 14 February 1984)

The effect of fluorine and chlorine implantation on the solid-phase epitaxial regrowth of amorphized $\langle 100 \rangle$ Si was studied in intrinsic and heavily boron doped material. Annealings were performed at 500 and 600 °C. Both F and Cl retard the regrowth rate at 500 °C. The growth rates are much faster in B-doped than in undoped Si. Complete regrowth in B-doped Si is obtained for all investigated doses of fluorine up to 5×10^{15} F/cm² at 600 °C for 30 min. The highest dose of chlorine (5×10^{15} Cl/cm²) stops the regrowth at this temperature.

I. INTRODUCTION

Shallow *p*-type doping of silicon by implantation of molecular boron halide ions such as BF₂⁺ and BCl₂⁺ has recently attracted much attention.^{1,2} Several advantages compared to the conventional B⁺ implantation have been inferred from experimental results on BF₂⁺ implantations: (i) Since the implantation energy for BF₂⁺ is higher than that for B⁺ to form an identical boron range distribution, larger and more stable ion beams can be obtained for BF₂⁺ implantation.³ (ii) For the implantation of heavy BF₂⁺ molecules, with doses above 1×10^{15} ions/cm², amorphous layers are formed at Si surface resulting in an efficient activation of boron during low-temperature recrystallization of these amorphous layers.⁴ (iii) *p*⁺-*n* junctions formed by BF₂⁺ implantation have low reverse leakage current.⁵ On the other hand, less satisfactory results have been obtained for other boron halides. As an example the electrical properties of Si heavily implanted with BCl₂⁺ are known to be poor.^{1,2}

Since the electrical activation of boron at low temperature is associated with the recrystallization of an amorphous surface layer formed during the implantation, the role that the halogen impurities play in the epitaxial regrowth process is of fundamental importance. Previous investigations have shown that impurities such as O, N, C or rare gas atoms Ne, Ar, and Kr retard the epitaxial growth rate in Si.⁶ Similar effects are expected and indeed observed for halogen impurities.⁴ Mainly from electrical measurements on molecular boron implantations; direct growth data are scarce. For the same reason, the influence of halogen impurities on the regrowth behavior of undoped Si crystals has not been explored.

In this study, we investigate the influence of ion-implanted F and Cl impurities on the recrystallization of amorphous Si in the low temperature regime where the solid-phase epitaxial regrowth is the prevailing crystallization mechanism. To provide useful data for applications of molecular boron implantations, the experiments were carried out on both intrinsic and heavily boron doped Si substrates. The epitaxial regrowth rates were determined by using back-scattering and channeling spectrometry.

^{a)} Permanent address: Semiconductor Laboratory, Technical Research Centre of Finland, Otakaari 5A, SF-02150 Espoo 15, Finland.

^{b)} Permanent address: Yokneam 20600, Israel.

II. EXPERIMENTAL PROCEDURES

The implantations were done into 3–10- μ m-thick epitaxial layers on $\langle 100 \rangle$ oriented Si substrates. Two different boron concentrations of the epilayers were used: (i) $C_B < 10^{16}$ B/cm³, (ii) $C_B \approx 1.7 \times 10^{20}$ B/cm³. The starting wafers were preamorphized at liquid nitrogen temperature with ²⁸Si⁺ implantations to a total dose of 3×10^{15} Si/cm² and to a depth of approximately 5000 Å. The high recrystallization rate observed in these amorphized layers upon annealing indicated that the ion beam was not contaminated by N₂ as sometimes anticipated for ²⁸Si⁺ implantations. To avoid channeling effects all implantations were performed 7° away from the main crystal axis. The preamorphized wafers were subsequently implanted to variable doses of ⁴⁷(SiF)⁺ or ³⁵Cl ions. ⁴⁷(SiF)⁺ rather than ¹⁹F⁺ was used to obtain the desired range distribution with a convenient implantation energy. The energies were chosen to give an approximately equal projected range of $R_p \approx 2000$ Å for both F⁺ and Cl⁺. This value was obtained by using Biersack's analytic approximation of projected ranges.⁷ The range of fluorine was calculated by assuming that the fraction $m_F/(m_{Si} + m_F)$ of the total energy E_0 of SiF⁺ ions was imparted to F⁺ where m_F and m_{Si} are the atomic masses of F and Si, respectively. The highest implantation dose was selected such as to yield a peak concentration that, in the boron doped substrates, corresponds to the atomic ratio of B/F = 1/2 or B/Cl = 1/2

TABLE I. Sequences of preamorphization and subsequent implantation of ¹⁹F and ³⁵Cl impurities into Si $\langle 100 \rangle$ substrates.

| Ion | Implantation temperature | Energy (keV) | Implantation dose (10 ¹⁵ /cm ²) | | |
|-------------------------------|--------------------------|--------------|--|---------|----------|
| | | | Reference | F-doped | Cl-doped |
| ²⁸ Si ⁺ | LN ₂ | 80 | 1.0 | 1.0 | 1.0 |
| | | 250 | 2.0 | 2.0 | 2.0 |
| SiF ⁺ | LN ₂ | 225 | ... | 1.0 | ... |
| | | | | or | |
| | | | | 2.0 | |
| | | | | or | |
| | | | | 5.0 | |
| ³⁵ Cl ⁺ | LN ₂ | 175 | ... | | 1.0 |
| | | | | | or |
| | | | | | 2.0 |
| | | | | | or |
| | | | | | 5.0 |

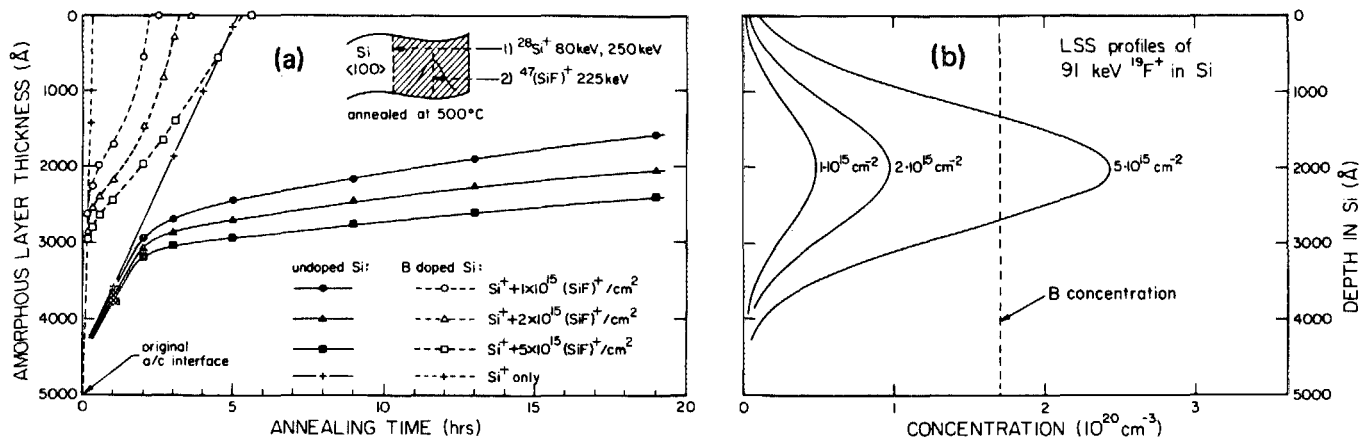


FIG. 1. (a) Regrowth characteristics of undoped and B-doped Si (100) amorphized with $^{28}\text{Si}^+$ irradiation and subsequently implanted with various doses of 225-keV $^{47}(\text{SiF})^+$; (b) calculated LSS profiles of fluorine.

normally obtained by molecular implantation of BF_2^+ or BCl_2^+ into Si. The details of the implantation procedures are given in Table I.

The implanted wafers were cut into small samples. The samples were then thermally annealed in a quartz tube vacuum furnace (residual pressure $< 10^{-6}$ Torr) at 500 °C for durations ranging from 10 min up to 19 h. After the recrystallization characteristics of these samples were determined, some of the samples were reannealed at 600 °C. To obtain an appropriate reference for the growth rates in SiF^+ and Cl^+ implanted crystals, samples implanted with Si^+ only were included in the same annealing procedure. The epitaxial growth rates were determined by measuring the thickness of the remaining amorphous layer in the annealed samples. These measurements were done by 1.5-MeV $^4\text{He}^+$ backscattering and channeling with a two-axis channeling goniometer and a Si surface barrier detector at a fixed 170° scattering angle. Transmission electron microscopy (TEM) was used to study the residual defects in fully regrown samples, and impurity profiles were taken by secondary ion mass spectrometry (SIMS) for some of the samples.

III. RESULTS

A. Effect of F

Figure 1(a) compares the regrowth characteristics of SiF^+ implanted samples to those implanted with Si only for thermal annealing at 500 °C. In this figure, the amorphous layer thickness obtained from channeling measurements is plotted as a function of the annealing time. The regrowth rate can be deduced from the slope of these curves. For samples implanted with Si only, the plots are straight lines described by constant growth rates of 14 and 300 Å/min for undoped and B-doped substrates, respectively. The data also show that the growth rates are significantly reduced by the presence of fluorine. In the undoped substrates, the regrowth slows down at a depth slightly less than 3000 Å. From the LSS distribution profiles in Fig. 1(b), one observes that for the lowest implantation dose (1×10^{15} F/cm²) this depth corresponds to a concentration of $\sim 3 \times 10^{19}$ F/cm³. Above this concentration, the growth rate decreases gradually to the level of ~ 1 Å/min. After 19 h annealing, the remaining amorphous layer is 1600 Å thick. For the higher

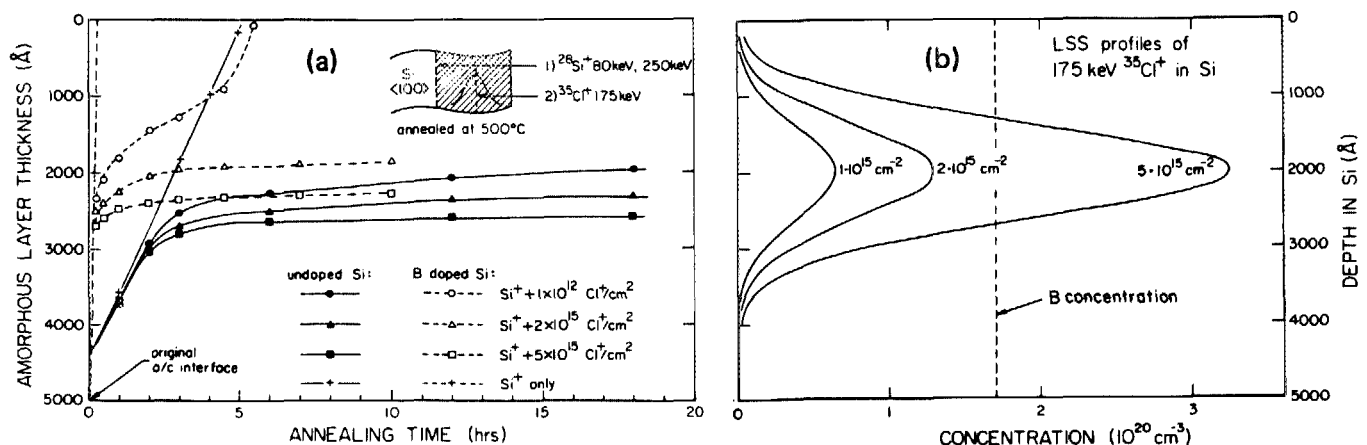


FIG. 2. (a) Regrowth characteristics of undoped and B-doped Si (100) amorphized with $^{28}\text{Si}^+$ irradiation and subsequently implanted with various doses of 175-keV $^{35}\text{Cl}^+$; (b) calculated LSS profiles of chlorine.

implantation doses, the reduction of the growth rate occurs at larger depth and the final growth rates through the fluorine peak are slightly lower than 1 Å/min. Due to the fluorine, the annealing times for complete regrowth become impractically long at this temperature.

The growth rates observed in boron doped samples are shown by the dashed lines in Fig. 1(a). Here again the regrowth slows down in the region of high fluorine concentration. The net growth, however, remains at the level of ~20 and ~8 Å/min for the lowest and the highest fluorine dose respectively. A complete regrowth of the amorphous layer is obtained within 5 h of annealing even for the highest implantation dose.

At 600 °C, the regrowth is completed in 30 min for all doses of fluorine implanted into B-doped samples. In the undoped substrates, the recrystallization is also complete except for the highest fluorine dose where the thickness of the remaining amorphous layer is approximately 950 Å.

B. Effect of Cl

Figure 2(a) shows the annealing characteristics of Cl⁺ implanted Si. As in the case of fluorine, the regrowth is severely retarded by the presence of chlorine. In undoped substrates, the growth is practically stopped at the depth below the maximum Cl concentration. Only the sample with the lowest Cl⁺ dose continues to grow with a rate of ~0.3 Å/min at the peak concentration of 6.5 × 10¹⁹ Cl/cm³. It should

be noted that the implantation profiles are steeper with higher peak concentrations than in the case of fluorine due to the smaller range straggling [see Fig. 2(b)].

The dashed lines in Fig. 2(a) further demonstrate the differences of SiF⁺ and Cl⁺ implanted samples. In boron doped Si, complete regrowth is obtained only for the lowest Cl dose (1 × 10¹⁵ Cl/cm²). At higher dose levels, the recrystallization is almost completely stopped. After 10 h annealing, the remaining amorphous layers are ~1900 and 2200 Å thick for Cl⁺ doses of 2 × 10¹⁵ and 5 × 10¹⁵ Cl/cm², respectively.

Annealing at 600 °C for 30 min produces similar results. The channeling spectra in Fig. 3 demonstrate the Cl⁺ dose dependence of the regrowth accomplished at that tempera-

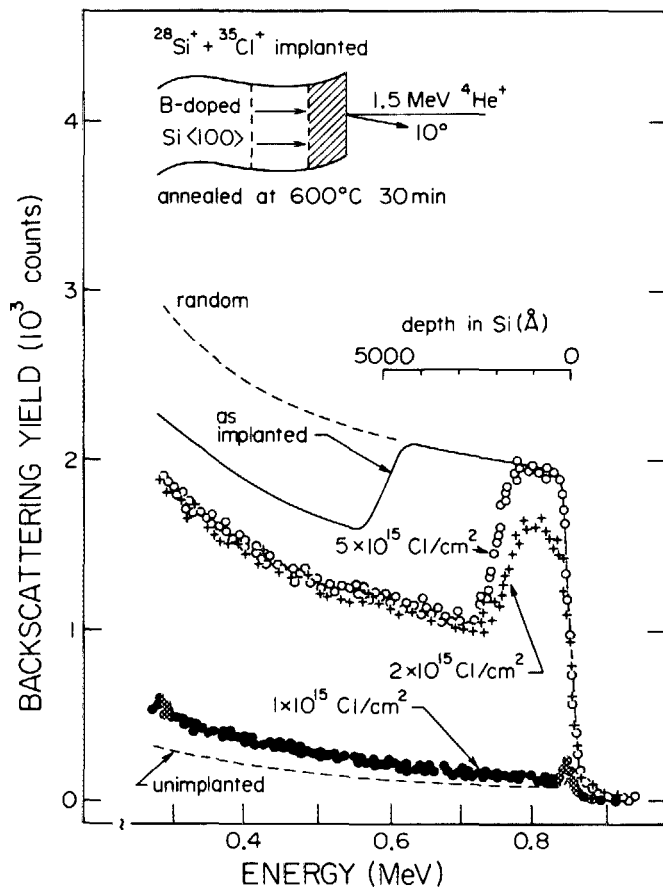


FIG. 3. Backscattering spectra for aligned beam incidence of B-doped Si implanted with 175-keV ³⁵Cl⁺ ions at various dose levels and subsequently annealed at 600 °C for 30 min. See text for details.

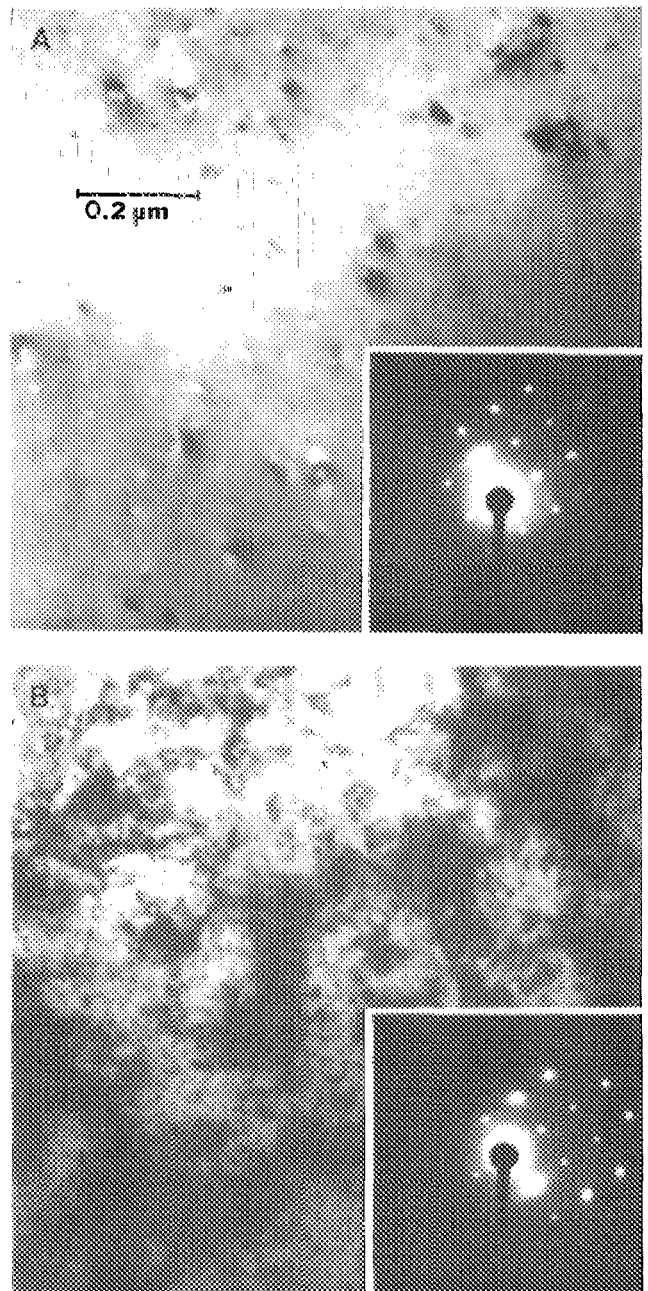


FIG. 4. TEM micrographs and electron diffraction patterns taken from B-doped Si samples implanted with (a) 1 × 10¹⁵ F/cm² and (b) 1 × 10¹⁵ Cl/cm² and subsequently fully regrown at 500 °C to the surface.

ture after 30 min. The lowest Cl^+ dose results in a complete regrowth of the amorphous layer whereas the highest dose halts the interface at the depth of 2000 Å. For the intermediate dose of $2 \times 10^{15} \text{ Cl/cm}^2$, imperfect epitaxial growth is obtained, as the reduced backscattering yield throughout the regrown surface layer indicates. Full recovery of crystallinity is obtained in this case after an additional annealing step of 1 h at 600 °C. The same annealing procedure does not produce any further regrowth in samples implanted with $5 \times 10^{15} \text{ Cl/cm}^2$ and the interface remains halted at the peak of the original Cl distribution.

A large number of growth defects were observed in the bright field TEM pattern taken from a fully grown boron doped sample with $1 \times 10^{15} \text{ Cl/cm}^2$ after 5½ h annealing at 500 °C [Fig. 4(b)]. The electron diffraction pattern from the same sample revealed partly amorphous or fine grained polycrystalline regions in some selected areas. In comparison, the TEM pattern from a F^+ implanted sample [Fig. 4(a)] shows a much lower concentration of defects and in the diffraction pattern there is no evidence for amorphous or polycrystalline regions. Samples without F or Cl showed no defects in TEM micrographs after a similar annealing treatment. In the backscattering spectra for aligned beam incidence (Fig. 3), this laterally nonuniform structure results in a slightly increased dechanneling yield. The size of the defects observed by TEM was small, typically < 100 Å and therefore they were difficult to identify.

IV. DISCUSSION

The regrowth rates we measured for undoped and for B-doped samples amorphized only by $^{28}\text{Si}^+$ irradiation are slightly higher than the corresponding values reported for undoped and ^{11}B implanted amorphized Si respectively at

500 °C.⁸ The regrowth in B-doped Si is approximately 20 times faster than in undoped Si. This value is in agreement with a previously observed enhancement factor of 25 in samples containing $(2-2.5) \times 10^{20} \text{ B/cm}^3$ and annealed at 500 °C.^{8,9}

A sharp decrease of the regrowth rate is observed in samples which have received an additional $(\text{SiF})^+$ or Cl^+ implantation. The depths at which the reduction in regrowth rate sets in for different implantation doses do not correspond to the same concentration of the original impurity distribution. Rather, the results suggest that considerable redistribution of halogen atoms occurs such that impurities accumulate at the advancing amorphous-crystalline interface. Since for epitaxial regrowth long range transport of Si is neither required nor expected at low temperatures, the growth rate should be affected by the local impurity concentration only. Without redistribution, the rate should accelerate past the peak of the implantation profile. Although some acceleration is observed for the low-dose implants in B-doped substrates, the regrowth curves are not symmetric with respect to the mean depth of the implantation profile. This further supports the view that accumulation at the interface occurs. This idea is also consistent with the results of Tsai *et al.*,¹⁰ who observed a "spike" in the fluorine profile moving toward the surface as the recrystallization proceeds at 550 °C. Since the fluorine is not very mobile at this temperature, the redistribution was attributed to accumulation at the amorphous-crystalline interface.

That an accumulation of impurities does, in fact, occur is convincingly demonstrated by the fluorine and chlorine depth distributions measured by SIMS (see Figs. 5 and 6). The location of the amorphous-crystalline interface as determined from Figs. 1(a) and 2(a) are indicated by a vertical line in Figs. 5(a) and 6(a). Within the accuracy of their depth

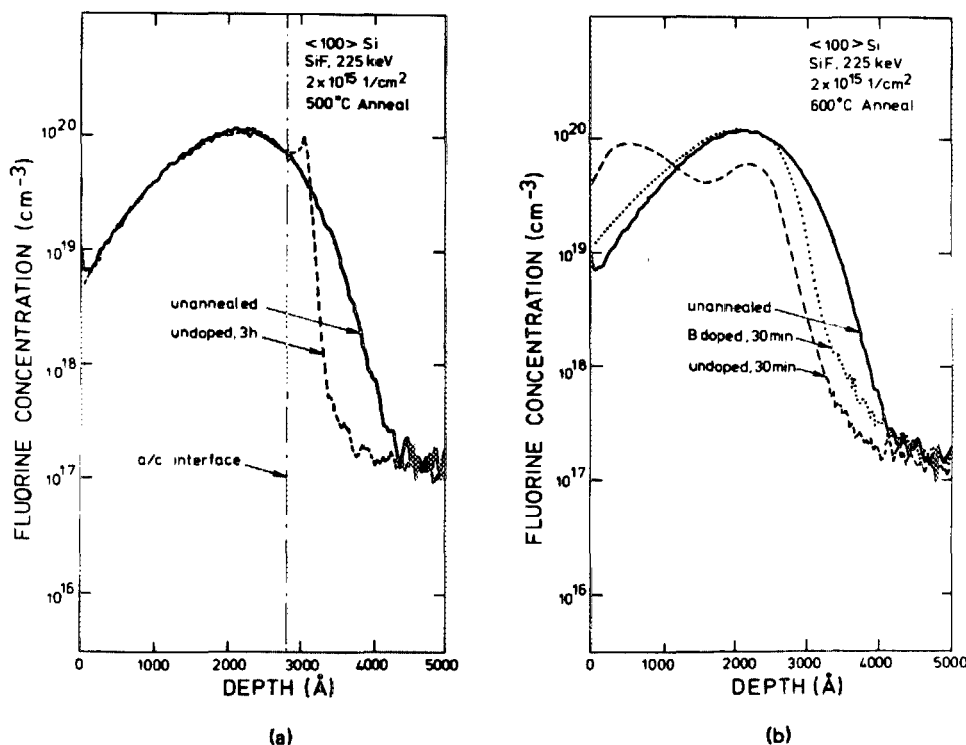


FIG. 5. SIMS depth profiles of fluorine in Si(100) wafers amorphized with $^{28}\text{Si}^+$ irradiation and subsequently implanted with a dose of $2 \times 10^{15} \text{ }^{47}(\text{SiF}^+)/\text{cm}^2$ and annealed at (a) 500 °C, (b) 600 °C.

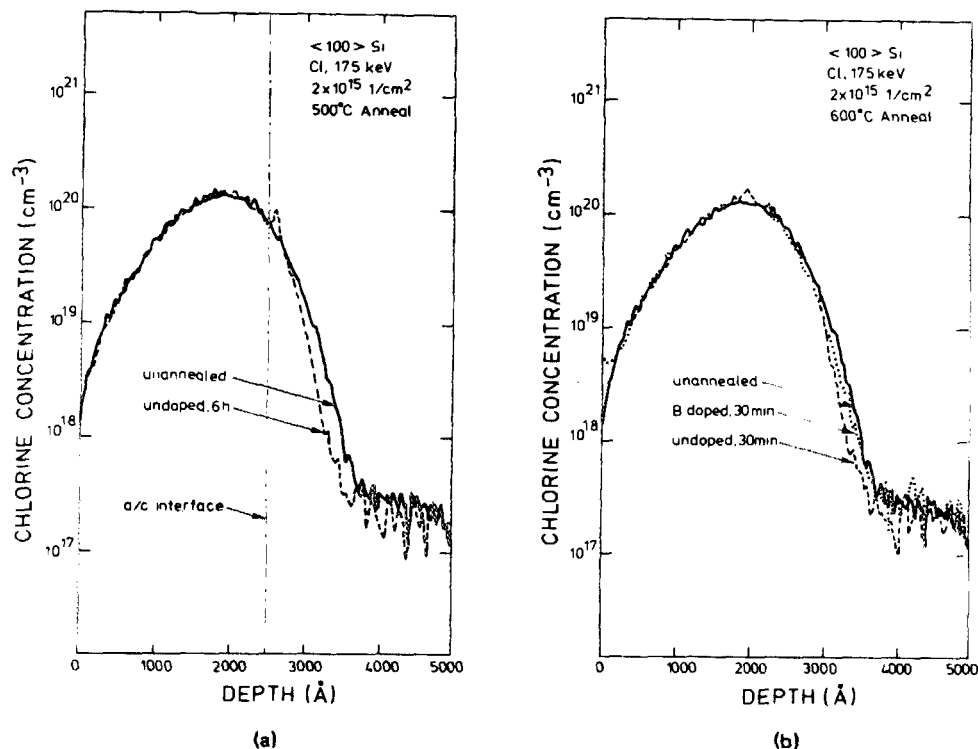


FIG. 6. SIMS depth profiles of chlorine in Si(100) wafers amorphized with $^{28}\text{Si}^+$ irradiation and subsequently implanted with a dose of $2 \times 10^{15} \text{ }^{35}\text{Cl}^+/\text{cm}^2$ and annealed at (a) 500 °C, (b) 600 °C.

scales, the SIMS spectra show a distinct peak at that location. It is also clear that F redistributes more than Cl does. The profiles for 600 °C annealing in Fig. 5(b) further shows that fluorine redistribution is more pronounced in undoped samples (that regrow slowly) than in B-doped samples (that regrow rapidly). At 600 °C, the analyzed fluorine samples were all fully regrown [Fig. 5(b)]; in the undoped chlorine sample, the regrowth had only progressed up to the peak of the original chlorine distribution. The as-implanted profiles in Figs. 5 and 6 are in good agreement with the profiles calculated from LSS theory and shown in Figs. 1 and 2.

As shown by Fig. 1(a), the growth rates in B-doped samples remain at a much higher level than in undoped Si for all implanted F doses. At the highest dose levels, the deceleration due to the fluorine overrides the acceleration by B and the resulting growth rate falls below the intrinsic growth rate [solid straight line in Fig. 1(a)]. The total growth velocity is a result of combined and opposite effects of B and F. The inflexion point of the growth curves for high implantation doses (2×10^{15} and $5 \times 10^{15} \text{ F/cm}^2$) roughly coincides with the peak of the F distributions. Accumulation of F appears to be significantly less in B-doped than in undoped substrates where the regrowth rate remains low even beyond the peak of F distribution. This result implies that the amount of accumulated F depends on the competition between the regrowth rate of the Si matrix and the rate of F accumulation at the interface. The enhanced regrowth rates in B-doped Si result in less accumulation in this case.

The retarding effect of Cl is much more pronounced than the effect of F. Actually, at the highest dose of $5 \times 10^{15} \text{ Cl/cm}^2$, the regrowth is completely stopped even at 600 °C. Since Figs. 5 and 6 show that Cl and F accumulate roughly equally, this means that for similar concentrations Cl influences the regrowth more than F. Beanland¹ observed that

large amounts of Cl implanted into Si together with B are retained in the crystal even after annealing at 1100 °C, whereas F introduced by a similar procedure is free to escape during high temperature anneals. In the same study, chlorine bubbles were observed in transmission electron micrographs after annealing at 800 °C. These observations support the idea that Cl has a lower mobility and stronger tendency to precipitate in Si than F. This general picture is consistent with our results.

The fact that for the lowest Cl dose ($1 \times 10^{15} \text{ cm}^{-1}$) the regrowth accelerates past the peak in the implanted distribution [see Fig. 2(a)] fits the model of a competition between rates of regrowth and impurity accumulation. Apparently, the regrowth in this case is fast enough to leave the accumulated impurities behind so that recrystallization can proceed to the surface.

The data presented here do not provide insight into the detailed mechanism of crystallization. For example, one could also explain the differences between F and Cl in the presence of B by different enhanced solubilities in Si. Whatever the details, it is clear that for molecular implantations of B, BF_2^+ is preferable to BCl_2^+ . In practical applications, a typical high-dose implantation of molecular boron ions into Si results in a peak halogen concentration in the order of 10^{20} – 10^{21} at./cm^3 . Our data show that Cl present at this concentration level may prevent the epitaxial recovery of the implanted layer. As a consequence, poor activation of boron should be expected for annealing at low temperatures.

V. CONCLUSIONS

The results presented here lead to the conclusion that the low temperature epitaxial regrowth of Si is severely affected by the presence of F or Cl. The effect can be attributed

to the accumulation of halogen impurities at the amorphous-crystalline interface advancing toward the surface. The difference between F and Cl implanted samples is significant. Complete regrowth in B-doped Si is obtained for all investigated doses of fluorine ($< 5 \times 10^{15}$ F/cm²) at 600 °C for 30 min. The highest dose of chlorine (5×10^{15} Cl/cm²) stops the regrowth even at this temperature. The poor regrowth behavior of Cl implanted Si can explain the unsatisfactory electrical properties usually observed in BCl₂⁺ implanted Si.

ACKNOWLEDGMENTS

We acknowledge Professor S. S. Lau (University of California at San Diego) for valuable discussions and L. Csepregi (Fraunhofer-Institut für Festkörpertechnologie, Federal Republic of Germany) for supplying the boron doped wafers. At Caltech the completion of this work was partially supported by the U. S. Department of Energy through an agreement with the National Aeronautics and Space Administration and monitored by the Jet Propulsion Laboratory, California Institute of Technology (D. R. Burger). The

SIMS work at the University of Illinois, Urbana-Champaign, was supported by the National Science Foundation under the MRL Grant DMR-80-20250.

¹D. Beanland, *Solid-State Electron.* **21**, 537 (1978).

²G. Fuse, T. Hirao, K. Inoue, S. Takayanagi, and Y. Yaegashi, *J. Appl. Phys.* **53**, 3650 (1982).

³H. Müller, H. Ryssel, and I. Ruge, *Ion Implantation in Semiconductors*, edited by I. Ruge and J. Graul (Springer, Berlin, 1971), p. 85.

⁴M. Y. Tsai and B. G. Streetman, *J. Appl. Phys.* **50**, 183 (1979).

⁵S. Prussin, *Ion Implantation in Semiconductors*, edited by S. Namba (Plenum, New York, 1975), p. 449.

⁶E. F. Kennedy, L. Csepregi, J. W. Mayer, and T. W. Sigmon, *J. Appl. Phys.* **48**, 4241 (1977).

⁷J. P. Biersack and J. F. Ziegler, *Ion-Implantation Techniques*, edited by H. Ryssel and H. Glawischnig (Springer, Berlin, 1982), p. 157.

⁸L. Csepregi, E. F. Kennedy, T. J. Gallagher, J. W. Mayer, and T. W. Sigmon, *J. Appl. Phys.* **48**, 4234 (1977).

⁹I. Suni, G. Göltz, M. G. Grimaldi, M-A. Nicolet, and S. S. Lau, *Appl. Phys. Lett.* **40**, 269 (1982).

¹⁰M. Y. Tsai, D. S. Day, B. G. Streetman, P. Williams, and C. A. Evans, Jr., *J. Appl. Phys.* **50**, 188 (1979).